European Conference on Optical Communication (ECOC) 2022 © Optica Publishing Group 2022

Challenges in Modeling Wideband Transmission Systems

André Richter[(1)], Gabriele Di Rosa[(1)], Igor Koltchanov[(1)]

[(1)] VPIphotonics GmbH, Carnotstr. 6, Berlin, Germany, andre.richter@vpiphotonics.com

Abstract *We discuss fiber link analysis challenges of ultra-wideband WDM transmission systems. Exploring an S+L band system, we demonstrate the importance of accounting for the wavelength dependence of the fiber characteristics, particularly the nonlinear effects. ©2022 The Author(s)*

Motivation

After an initial deployment period in the early 2000s, we experience again increased interest in ultra-wideband (UWB) wavelength division multiplexing (WDM) systems utilizing the combined S-C-L band. These efforts are triggered by the steady growth of network traffic and the continued utilization of existing fiber infrastructure as long as economically and operationally possible. UWB-WDM represents a cost-effective mid-term solution when combined with spectrally efficient high-order modulation formats for increased channel capacity until new technologies become commercially attractive[1].

The UWB-WDM channels cover an extensive spectral range and, consequently, are impacted differently by fiber propagation effects. Moreover, as appropriate solutions are not available at all desired wavelengths, the application of standard C-band transceivers outside their nominal wavelength operational range[2],[3] moves into focus, setting additional wavelength-dependent restrictions on the design and operation of UWB systems. Geometrical and probabilistic constellation shaping combined with rate-adaptive Forward-Error Correction (FEC) codes and correspondingly adapted new types of Digital Signal Processing (DSP) algorithms enable the deployment of flexible transceivers, which may account for the wavelength-dependent nature of the UWB end-to-end channels[4].

The application of numerical simulations and (semi-)analytical modeling approaches for the design, analysis, and optimization of UWB systems needs to account for these aspects. Moreover, tracking hundreds of signals, their properties, and critical interactions along the complete transmission link represents an additional challenge. While focusing on the fiber link analysis of UWB-WDM systems, we discuss and exemplify some of these considerations through numerical results obtained for an S+L band system.

Fiber Link Analysis of UWB Systems

Numerical solutions of the Generalized Nonlinear Schrödinger Equation (GNLSE, for linear polarization only) and Manakov-PMD Equation (MPE, arbitrary polarization) provide valuable insight into the signal, noise, distortions dynamics and interactions[5]. They can be used to derive, verify, and improve (semi-)analytical nonlinear fiber models, such as the ones based on the Gaussian Noise (GN) approximation[6],[7].

Accurate predictions require considering the wavelength dependence nature of the fiber parameters, as illustrated in Fig. 1. Furthermore, polarization-dependent nonlinear interactions due to the Kerr effect and inter-channel stimulated Raman scattering (ISRS) can impact the signal performance and must be assessed carefully. These aspects set stringent requirements for a robust and flexible numerical fiber propagation model. Among the criteria are numerical solvers of high precision, flexible spectral resolution, robust iterative boundary value solvers for bidirectional power analysis, adaptive split-step size management[8],[9], control of polarization scattering sections and their correlation[10], and of nonlinear interaction bandwidths.

Especially difficult for modeling UWB systems is the high demand for memory and simulation time. Combining both detailed and coarse multiple signal representations, approximating signal dynamics and interactions, and the careful isolation of fiber propagation effects can limit the impact of these restrictions[11],[12]. Using a single frequency band (SFB) to represent the complete UWB-WDM spectrum allows calculating all interactions with the highest accuracy at the expense of simulation time and memory. The frequency decomposition concept enables a multiple frequency band (MFB) representation, usually providing computation resource savings when investigating systems with spectral gaps. Time and memory demand can be decreased further by utilizing time-averaged signal representations when investigating purely power-related or semi-analytically derivable interaction processes[13]. The Mean Field approach[14] enables the combined consideration of these signal representations in the fiber propagation equations. With this, various effects can be switched on and off, wavelength-dependent link characteristics accounted for, and computational resources and the numerical accuracy controlled[15].

The parallelization of numerical solvers and utilization of General-Purpose Graphical Processor Units (GPGPU) with double-precision accuracy (further referred to as GPU) are other essential tools for making wideband systems simulations feasible. Even though GPU-assisted computations can reach a 15x to 50x speedup over CPU-only computations[16], they may still take considerable time, especially when exploring a large parameter space and performing multiple simulations. The overall simulation time can be estimated based on a single-span reference run and scaling its time with the number of symbols, signal power, effective fiber length, simulation bandwidth, number of spans, and a computer-specific correction factor. Besides performance, an important aspect for the GPU choice is the required memory size. Its demand is $\approx KN_{sa}32$ B, with $K \sim 4...14$ accounting for the number of signal copies taken in memory considering the various fiber effects, where N_{sa} represents the number of simulated samples. Typically, $N_{sa} = \Pi_k k^{M_k}$, with M_k being integers and k low primes to benefit from the speed advantage of the Fast Fourier Transform. Using only $k = 2$ can lead to excessive sizes of N_{sa}, while a mix of different prime bases may avoid this problem[17][18]. Of course, N_{sa} needs to be adjusted carefully, considering relevant fiber effects[5],[18], the convergence of DSP algorithms, and the statistical nature of system performance measures.

Nonlinearities in an S+L Band System

As an example, we simulate the transmission of two WDM combs, centered around 1500 and 1600 nm, over a low water peak (LWP) fiber in VPIphotonics Design Suite 11.2. This scenario, characterized by two widely separated optical bands, represents an interesting case to demonstrate the capabilities of the MFB approach to consider the wavelength-dependency of the generation of nonlinear distortions (NLIN) effectively.

Fig. 1 depicts the variability of the fiber nonlinearity parameter (γ), effective area (A_{eff}), attenuation coefficient (α), and dispersion coefficient (D) for $\lambda_0 = 1550$ nm. We can observe that they all vary by $> 10\%$ in the considered 140 nm bandwidth, highlighting the importance of considering their wavelength dependence when calculating the NLIN terms.

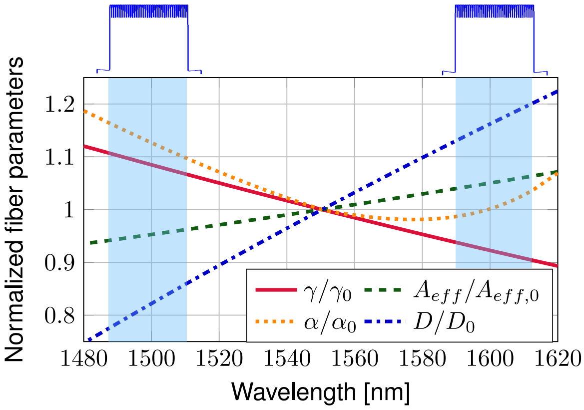

Fig. 1: Fiber parameters normalized to their respective values at $\lambda_0 = 1550$ nm. Values based on measurements and specifications of a SMF-28e LWP fiber.

While the attenuation and dispersion profiles are commonly considered for accurate analysis of C-band systems, γ is often approximated as a single value. This assumption is motivated by the small variability of γ ($\pm 3\%$ range) in that band. However, this approximation introduces a more significant inaccuracy when simulating UWB-WDM systems. Assuming the nonlinear index n_2 is a constant[19], $\gamma(\lambda) = \frac{2\pi n_2}{\lambda A_{eff}(\lambda)}$. As a result of the inverse dependency of γ on wavelength and effective area, we see from Fig. 1 that $\gamma_{1600\text{ nm}} \approx 1.176\gamma_{1500\text{ nm}}$ and thus, exhibits a much larger variability than for C-band systems.

In this scenario, the MFB representation provides a great tool to capture the wavelength dependency of the nonlinear coefficient while providing a consistent simulation speedup. The solution of coupled MPEs allows calculating the intra-band nonlinear terms of the k-th band efficiently, considering the local γ_k and the inter-band nonlinear interactions with a second j-th band through $\gamma_{kj} = \frac{2\pi n_2}{\lambda_j A_{eff}(\lambda_j,\lambda_k)}$, where $A_{eff}(\lambda_j, \lambda_k)$ describes the overlap of the interacting modal fields. To test the impact of the wavelength-dependency of γ, we simulate a multi-span transmission system either considering $\gamma(\lambda)$ as from Fig. 1 or enforcing $\gamma_0 = 1.3085$ 1/W/km at all wavelengths.

The transmitted signal consists of two WDM combs, with 41 channels each on a regular 75 GHz grid. The channels carry 16-QAM modulated signals with a symbol rate of 64 Gbaud and an optical power of $P_{ch} = 0$ dBm. We consider

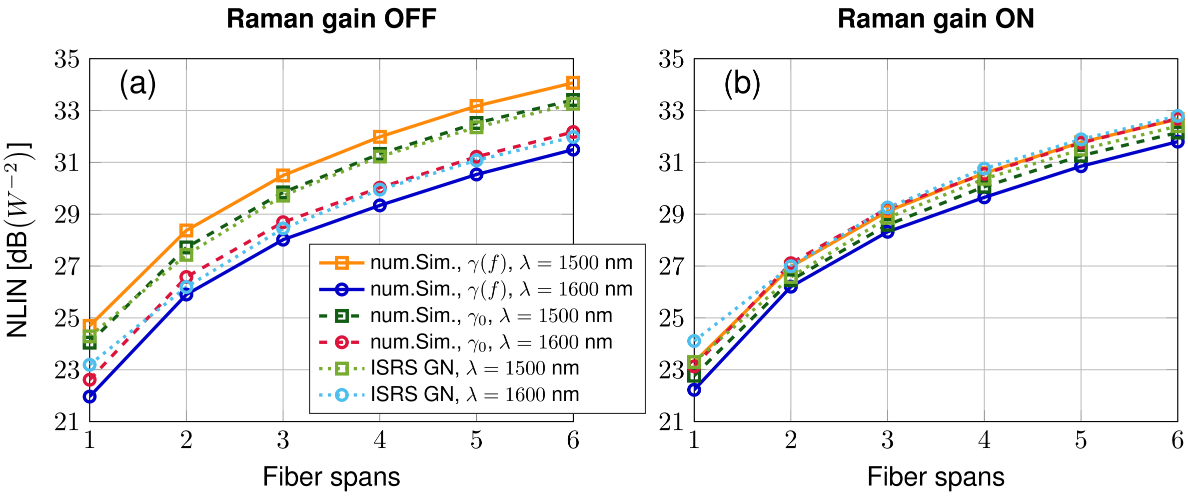

Fig. 2: NLIN estimated through numerical simulations, with and without considering the wavelength-dependency of γ, and with the analytical formulation of the ISRS GN model[7]. Results neglecting (a) and including (b) ISRS.

fixed sequences of 2^{15} symbols for each simulation, and perform pulse shaping through a raised-cosine filter with zero roll-off. The transmitted signals are then propagated over up to 6 spans of 80 km LWP fiber, characterized by the following parameters at $\lambda_0 = 1550$ nm: $\alpha_0 = 0.1903$ dB/km, $D_0 = 16.128$ ps/nm/km, $A_{eff,0} = 76.9$ μm^2, and their wavelength dependence from Fig. 1. After each span, an ideal, noiseless amplifier restores the optical power of each channel, taking into account the Raman power transfer. Ideal chromatic dispersion compensation and inversion of the Jones matrix of the link are performed after fiber propagation to consider only the impairments arising from the fiber nonlinearity. Finally, the channels under test, centered around 1500 and 1600 nm, are filtered through ideal rectangular filters with 64 GHz bandwidth before coherent reception. At this point, the digitized signals are scaled and rotated to estimate the variance of the NLIN from the received constellations using a statistical quantification method[20].

Fig. 2 shows the estimated NLIN variance, normalized by P_{ch}^3, for the central channels of the two bands, at 1500 and 1600 nm, respectively. The results are obtained through numerical simulations (w/ and w/o considering the wavelength dependency of γ) and by using the ISRS GN model (including the NLIN dependence on the modulation-format[7]). Fig. 2 (a) shows the results when neglecting ISRS, representing a scenario of two weakly interacting bands where the NLIN generation is dominated by intra-band single- and cross-channel interference. In these conditions, numerical simulations with fixed γ_0 and the analytical method provide comparable NLIN estimations, validating their operation. However, when accounting for $\gamma(\lambda)$, the values obtained are larger at 1500 nm and smaller at 1600 nm, consistently with the trend observed in Fig. 1.

While these results corroborate the validity of the analysis methods, considering ISRS represents a more interesting practical scenario, leading to the results in Fig. 2 (b). We observe that ISRS reduces the NLIN variance gap between the two bands thanks to the power transfer from lower to higher wavelength, which reduces the difference in NLIN generation given mainly by the wavelength-dependent dispersion coefficient. The numerical analysis with fixed gamma and the analytical calculation provide comparable results again. However, considering $\gamma(\lambda)$ has a direct impact on the NLIN generation and an indirect one as the Raman power transfer, and thus the signal power profile is modified. As a result, we observe a worst-case discrepancy of ≈ 0.9 dB between the numerical results obtained at 1600 nm w/ and w/o considering the wavelength-dependence of γ, highlighting its importance.

Conclusions

We presented essential aspects that make the design of ultra-wideband WDM systems a very demanding modeling task. While focusing on the fiber link analysis of such systems, we provided important modeling and simulation guidelines. Exploring an example S+L band system, we numerically calculated the nonlinear distortions in both bands.

Acknowledgements

This work is funded by the EU under H2020-MSCA-ITN-2018, grant 814276 (WON) and the German Federal Ministry of Education and Research, grant 16KIS0993 (OptiCON).

References

[1] A. Ferrari, A. Napoli, J. K. Fischer, *et al.*, "Assessment on the achievable throughput of multi-band ITU-T G. 652. D fiber transmission systems", *Journal of Lightwave Technology*, vol. 38, no. 16, pp. 4279–4291, 2020.

[2] G. Di Rosa, R. Emmerich, M. Ribeiro Sena, *et al.*, "Characterization, monitoring, and mitigation of the i/q imbalance in standard c-band transceivers in multi-band systems", *Journal of Lightwave Technology*, pp. 1–1, 2022. DOI: 10.1109/JLT.2022.3154888.

[3] T. Kato, S. Watanabe, T. Yamauchi, *et al.*, "Whole band wavelength conversion for wideband transmission", in *2021 Optical Fiber Communications Conference and Exhibition (OFC)*, 2021, pp. 1–3.

[4] L. Galdino, A. Edwards, W. Yi, *et al.*, "Optical fibre capacity optimisation via continuous bandwidth amplification and geometric shaping", *IEEE Photonics Technology Letters*, vol. 32, no. 17, pp. 1021–1024, 2020. DOI: 10.1109/LPT.2020.3007591.

[5] G. P. Agrawal, "Nonlinear fiber optics", in *Nonlinear Science at the Dawn of the 21st Century*, Springer, 2000, pp. 195–211.

[6] A. Carena, G. Bosco, V. Curri, Y. Jiang, P. Poggiolini, and F. Forghieri, "Egn model of non-linear fiber propagation", *Optics Express*, vol. 22, no. 13, pp. 16 335–16 362, 2014.

[7] D. Semrau, E. Sillekens, R. I. Killey, and P. Bayvel, "A modulation format correction formula for the gaussian noise model in the presence of inter-channel stimulated raman scattering", *Journal of Lightwave Technology*, vol. 37, no. 19, pp. 5122–5131, 2019. DOI: 10.1109/JLT.2019.2929461.

[8] C. Francia, "Constant step-size analysis in numerical simulation for correct four-wave-mixing power evaluation in optical fiber transmission systems", *IEEE Photonics Technology Letters*, vol. 11, no. 1, pp. 69–71, 1999.

[9] O. V. Sinkin, R. Holzlöhner, J. Zweck, and C. R. Menyuk, "Optimization of the split-step fourier method in modeling optical-fiber communications systems", *Journal of Lightwave Technology*, vol. 21, no. 1, p. 61, 2003.

[10] G. Biondini, W. L. Kath, and C. R. Menyuk, "Importance sampling for polarization-mode dispersion", *IEEE Photonics Technology Letters*, vol. 14, no. 3, pp. 310–312, 2002.

[11] A. Lowery, O. Lenzmann, I. Koltchanov, *et al.*, "Multiple signal representation simulation of photonic devices, systems, and networks", *IEEE Journal of Selected Topics in Quantum Electronics*, vol. 6, no. 2, pp. 282–296, 2000.

[12] A. Richter, "Modelling high-capacity nonlinear transmission systems", in *WDM Systems and Networks - Modeling, Simulation, Design and Engineering*, Springer, 2012, pp. 13–61.

[13] H. Louchet, N. Karelin, and A. Richter, "Modelling high-capacity nonlinear transmission systems", in *Optical Communication Systems: Limits and Possibilities*, CRC Press, 2019, pp. 1–61.

[14] T. Yu, W. Reimer, V. Grigoryan, and C. Menyuk, "A mean field approach for simulating wavelength-division multiplexed systems", *IEEE Photonics Technology Letters*, vol. 12, no. 4, pp. 443–445, 2000.

[15] VPIphotonics, "Universal fiber module reference", in *VPIphotonics Design Suite*, 2022.

[16] N. Karelin, G. Shkred, A. Simonov, S. Mingaleev, I. Koltchanov, and A. Richter, "Parallel simulations of optical communication systems", in *2014 16th International Conference on Transparent Optical Networks (ICTON)*, IEEE, 2014, pp. 1–4.

[17] M. Frigo and S. G. Johnson, "The design and implementation of fftw3", *Proceedings of the IEEE*, vol. 93, no. 2, pp. 216–231, 2005.

[18] P. Serena, C. Lasagni, S. Musetti, and A. Bononi, "On numerical simulations of ultra-wideband long-haul optical communication systems", *Journal of Lightwave Technology*, vol. 38, no. 5, pp. 1019–1031, 2019.

[19] K. S. Kim, R. H. Stolen, W. A. Reed, and K. W. Quoi, "Measurement of the nonlinear index of silica-core and dispersion-shifted fibers", *Optics Letters*, vol. 19, no. 4, pp. 257–259, DOI: 10.1364/OL.19.000257.

[20] G. Di Rosa, S. Dris, and A. Richter, "Statistical quantification of nonlinear interference noise components in coherent systems", *Optics Express*, vol. 28, no. 4, pp. 5436–5447, 2020.